ChemComm

Accepted Manuscript

This article can be cited before page numbers have been issued, to do this please use: Y. Niu, T. He, J. Song, S. Chen, X. Liu, Z. Chen, Y. Yu and S. Chen, *Chem. Commun.*, 2017, DOI: 10.1039/C7CC02555F.

ROYAL SOCIETY OF CHEMISTRY

rsc.li/chemcomm

View Article Online
DOI: 10.1039/C7CC02555F

Journal Name

COMMUNICATION

A new AIE multi-block polyurethane copolymer material for subcellular microfilaments imaging in living cells

Received 00th January 20xx,
Accepted 00th January 20xx

DOI: 10.1039/x0xx00000x

www.rsc.org/

Yu-qing Niu,[abc] Tao He,[d] Jun Song,[b] Si-ping Chen,[c] Xiang-yu Liu,[a] Zhi-gang Chen,[a] Ying-jie Yu,*[e] and Shi-guo Chen*[a]

A multi-block fluorescent amphiphilic polyurethane copolymer (TPE-PU), self-assembling into hairy, water-souble micelles, is used as the subcellular microfilaments probe in living cells.

As the major component of the cytoskeleton system, the protein actin forms dynamic microfilament systems, providing cells with mechanical support and driving forces for movement.[1] Specific targeting and binding of biomolecules or fluorescent materials to the microfilaments in living cells is a key research point in the biological field, as microfilaments contribute to numerous important biological processes such as cell dividing, membrane vesicles internalizing, environmental forces sensing, and moving over surfaces.[2] Currently, to realize specificity in imaging microfilaments in living cells, numerous fluorescent probes are developed as bioconjugates with actin specific peptide, actin antibody, alkaloid, and actin specific drugs.[3-6] However, cellular internalization of these actin labelling bioconjugates requires sophisticated cellular labelling techniques such as electroporation, microinjection and cell membrane permeabilization which deliver these bioconjugates into living cells owing to inefficient living cell membrane permeability of these fluorescent materials.[7-9] Another method is using fluorescent protein (GFP)-actin fusion proteins, which can be integrated into actin filaments after delicate transfection to achieve imaging actin in living cell.[10] But these strategies need multiple operation steps, which may alter the cell states and increase the imaging complexity.[11] Moreover, intrinsic disadvantages of these fluorescent probes, such as low photobleaching threshold for conventional organic dyes and GFP, and cytotoxicity for quantum dot (QD), greatly limit their applications in effective long term use and three-dimensional imaging.[12]

Motivated by the fact that fluorescent nanoparticles with size of 50-300 nm diameter could be efficiently internalized by living cells,[13,14] there is growing interest in developing fluorescent nanoparticles as probes for cellular imaging.[15-17] Tetraphenylethene (TPE) is archetypical aggregated-induced emission (AIE) fluorogen,[18,19] which has been extensively used for the design and use as cellular imaging fluorescent probes. The easy introduction of functional groups into TPE and its unique solid state emission properties make it possible for the construction of TPE containing copolymer probes for specific imaging of cells and intracellular macromolecules.[18-20] The microfilament protein actin is a rigid polymer molecule involved in a variety of fundamental biological processes,[21,22] hence it is highly necessary to explore a flexible and efficient fluorescent probe to reveal its structural, biochemical, and dynamic features.[23,24]

Herein, we functionalized TPE with two reactive hydroxyl (OH) groups (TPE-2OH), and then we designed and synthesized an AIE linear fluorescent block polyurethane copolymer probe based on TPE-2OH, polycaprolactone (PCL)-diol, and poly (ethylene glycol) (PEG) (abbreviated as TPE-PU) that can specifically bind to microfilaments in living cells. The polyurethane copolymer probe TPE-PU consisted of three chemically distinct polymers covalently

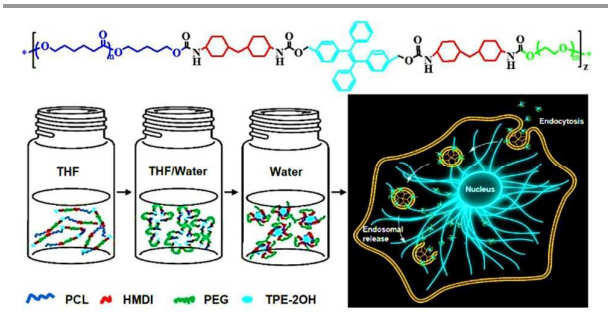

Fig. 1 Structure of the TPE-PU probe and schematic illustration of the TPE-PU nanoparticles forming process as well as the mechanism of subcellular microfilaments imaging in living cells.

[a] Nanshan District Key Lab for Biopolymers and Safety Evaluation, Shenzhen Key Laboratory of Polymer Science and Technology, Guangdong Research Center for Interfacial Engineering of Functional Materials, College of Materials Science and Engineering, Shenzhen University, Shenzhen 518060, PR China.
[b] Key Laboratory of Optoelectronic Devices and Systems of Ministry of Education and Guangdong Province, College of Optoelectronic Engineering, Shenzhen University, Shenzhen 518060, PR China.
[c] Shenzhen University Health Science Center, Shenzhen 518060, PR China.
[d] Multidisciplinary Research Center, Shantou University, Shantou, Guangdong 515063, China.
[e] Department of Materials Science and Engineering, Stony Brook University, Stony Brook, NY 11794, USA
[f] †Electronic Supplementary Information (ESI) available: Experimental section. See DOI: 10.1039/x0xx00000x

View Article Online
DOI: 10.1039/C7CC02555F

bonded together. Moreover, their constituent linear blocks of TPE-2OH, PCL-diol and PEG were chemically incompatible hence tend to demonstrate a flexible linear block structure in the block-selective solvent (Fig. 1). The PCL-diol segments served as the hydrophobic and rigid part, which, along with the fluorophore TPE-2OH segments, underwent fluorescence resonance energy transfer to show an aggregated polymer binding state. Soft PEG segments were inserted between hydrophobic PCL-diol and TPE-2OH segments to finetune the hydrophilicity and flexibility of the block copolymer. We showed here TPE-PU copolymer could be a good candidate as intracellular microfilament fluorescent probe for analysing the performance of the living cell microfilaments via specific imaging. In addition, cell uptake efficiency, photo-stability, and imaging simplicity, are superior to that of commercially available probe phalloidin.

The TPE-PU was synthesized by the mutual coupling reaction of terminal hydroxyl groups in PCL-diol, and TPE-2OH with terminal isocyanate groups from PEG-diisocyanate, as described in Fig. S1-2. By keeping the stoichiometric ratio of HMDI, PCL-diol, PEG and TPE-2OH at a molar ratio of 11:5:5:1, we obtained a series of linear TPE-PUs. The chemical structure and composition of the TPE-PU were analysed by ^{1}H NMR (Fig. S3). All the proton signals, belonging to PCL-diol, PEG, TPE-2OH and urea linkages can be clearly confirmed. The number-average molecular weight (M_n) of these TPE-PU polymers was ranging from 40.5 to 44.9 kDa with relatively narrow polydispersity indexes ranging from 1.39 to 1.61 (Table S1). Since different TPE-2OH segments were attached to the polyurethane chain, the AIE attribute of TPE-2OH enabled synthesis a series of linear TPE-PU copolymers with different fluorescence degree of labelling (DL). Here, the photoluminescence (PL) intensity of the TPE-PU increased as the PEG weight fraction decreased (Fig. 2A), which can be easily explained by the decline in PEG weight fraction, whilst keeping the other components constant. Moreover, the absorption spectrum of the TPE-PUs had one maximum peak at 360 nm, and their PL spectrum had a maximum peak at 505 nm, which is beneficial for confocal laser scanning microscope (CLSM) and fluorescence microscope for imaging. Furthermore, the appearance of the obtained TPE-PU films was changing from transparent to opaque milky white as the PEG content decreased and the TPE content increased. The difference in DL could result in different imaging ability. The TPE-PU films with different DL were excited by a UV light; they could emit light from blue, bright blue-green to greenish fluorescence, respectively (Fig. 2B). The higher the TPE-2OH content of the copolymers was, the stronger the light emission would be. Taken together, this revealed that the TPE-PUs were AIE active copolymers[25]. The AIE behaviour of a representative-PU sample was further researched in their solution state. As shown in Fig. S4, as the phenyl rings of TPE-2OH underwent active intra-molecular rotations in THF, there was almost no PL signal. Nevertheless, when large quantities of water (f_w > 60 Vol %) were admixed with THF, the linear TPE-PU copolymer chains spontaneously aggregated to form nanoparticles in THF/water mixture-solvents. Therefore, the TPE fluorophores started to radiate. When the THF/water mixture-solvents reached an f_w at 90 vol %, the PL intensity (I) of TPE-PU-1000 became ~ 1000-fold stronger than that in the THF solvent (I_0), indicating increasing clustering of the TPE-PU chains. As shown in Fig. S5, when the linear TPE-PU chains aggregated together, TPE-PU formed spherical nanoparticles with a core-shell structure with an average diameter of 30 ± 3 nm in pH 7.4, which possibly consisted of a dark interior core (hydrophobic and rigid PCL-diol and TPE-2OH segments) and a grey exterior shell (hydrophilic and flexible PEG segments). The restriction of the intramolecular rotation in TPE-PU impeded non-radiative decay channels to form radiative transition, hence, it contributed to the assembled fluorogenic molecules which emit high fluorescence (Fig. 1 and S5).

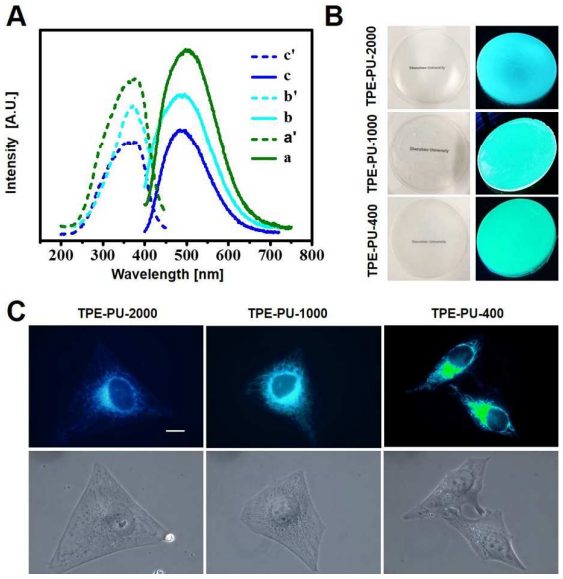

Fig. 2 Fluorescent characterizations of TPE-PUs. (A) Fluorescence spectrum of TPE-PUs in their solid films state. a, b, c, emission wavelength. a', b', c', excitation wavelength. a, a', TPE-PU-2000, b, b', TPE-PU-1000, c, c', TPE-PU-400. (B) Photographs of various TPE-PU films taken under room lighting and UV illumination. (C) Fluorescent image of the HeLa cells cultured in the presence of various TPE-PU nanoparticles with different DLs for 45 min at 37 ℃. [TPE-PU]=1 × 10^{-3} mg/mL, pH=7.4. Scale bar, 10μm (applicable to all images).

As the TPE-PU nanoparticles had flexible and hydrophilic PEG segments in their nanoparticle shell,[26,27] flexible chains with extended conformations when immersed in water. To demonstrate this, various TPE-PU nanoparticles were put in PBS solution at pH 7.4 for 1 h, the transmission electron microscopy (TEM) was then employed to study the morphology of the TPE-PU nanoparticles. As shown in Fig. S6, TPE-PU-400 exhibited core-shell nanoparticles with very smooth surface, and the PEG chains in the grey exterior shell stably wrapped the dark interior core. However, hydrophilic PEG chains could not exhibit flexible chain with extended conformations in the PBS solution, indicating that insertion of short PEG segment in the repeating units of the TPE-PU copolymer cannot improve the molecular conformation. In contrast, the PEG chains in the TPE-PU-1000 shell became transparent elastic filament, which were wrapped around its

View Article Online
DOI: 10.1039/C7CC02555F

hydrophobic dark interior core, suggesting the PEG chains could show extended chain conformations in PBS solution. The main reason was the conformation change of the PEG molecules on the nanoparticle surface. PEG chains solubilized easily and attained extended chain conformations due to their hydrophilicity and flexibility. The longer the PEG-segments, the more diffuse is the transition from the particle to the surrounding vacuum. Due to the different corona sizes, which depending on the PEG-segment lengths of 2.3/5.8/11.3 nm for PEG 400/1000/2000, respectively. As these segments are anchored on both ends, however, the realistic thickness of the corona is at most half of that value. Incidentally, these values seem to roughly agree to the width of the diffuse transition in Fig. S6, although this image was taken in vacuo and, hence, without solubilisation of the corona. The XRD analysis of the crystalline of TEP-PU copolymers showed PEG chains were extended in PCL crystalline lamellae to improve the flexibility and elasticity of the copolymers as the PEG content increased in the obtained copolymers (Fig.S7).

The AIE effect of the obtained TPE-PUs could be used as bio-probes for living cell imaging. HeLa cells were co-cultured with various TPE-PUs nanoparticles at pH 7.4 for 45 min, and their intracellular distribution were investigated by fluorescence microscopy. It was demonstrated in Fig. 2C that TPE-PU nanoparticles were readily internalized by HeLa cells and specifically bind to their intracellular microfilaments. When the living HeLa cells were cultured in the presence of TPE-PU with a DL of 1.489 mol %, the TPE-PU-2000 nanoparticles specific binding on the microfilaments emitted weak blue fluorescence. The microfilaments connect to filament bundles and form a filament network in the HeLa cell. However, due to the weak fluorescence intensity, we could not observe the fine microfilaments within the cellular cytosol (Fig. 2C). When the DL of the TPE-PU-1000 was increased to 1.838 mol %, the TPE-PU-1000 nanoparticles were uniformly distributed in the cytosol, and a clear blue green fluorescence intracellular microfilament network structure was observed (Fig. 2C). This may be due to the PEG extended chain conformations in the TPE-PU-1000 nanoparticles shells, which could enable real-time tracking of the microfilaments dynamic movements in viable cells. Very bright green blue fluorescence was emitted from the cytosol of HeLa cells stained by the TPE-PU-400 nanoparticles with a DL of 2.108 mol % (Fig. 2C). Compared to the TPE-PU-1000 and TPE-PU-2000 nanoparticles, the fluorescence light intensity was enhanced, however, the TPE-PU-400 nanoparticles cannot specifically bind to the intracellular microfilament bundles and network owing to low molar mass of the PEG-segments not long enough to be fully solubilized in the cell cytoplasm, as the hydrophobic shell is not sufficiently concealed by the short PEG-segments. This more hydrophobic surface of TPE-PU-400 nanoparticles tends to cause particles agglomeration in the cytosol (Fig. 2C).As the fluorescence intensity is too strong or low is not conductive to the microscopic observation of intracellular microfilaments, we chose TPE-PU-1000 with a DL of 1.838 mol % as the optimal microfilament bio-probe for living cell imaging. This intracellular microfilament specific imaging behaviour is of particular interest for the study of microfilament cytoskeleton in living cells.

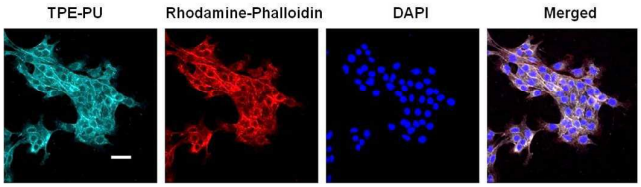

Fig. 3 The sub-cellular microfilaments colocalization of TPE-PU and Rhodamine Phalloidin in rat glial cells. The excitation/emission of TPE-PU (sample: TPE-PU-1000), Rhodamine Phalloidin, and DAPI lines was 364/470-505 nm, 543/565-620 nm, and 341/450-460 nm, respectively. Bar scale 20 μm (applicable to all images).

To further demonstrate whether our obtained AIE-attribute TPE-PU-1000 copolymer can specifically localize and image the subcellular microfilaments in other living cell lines, we incubated rat glial cells, a cell widely distributed in the central nervous system of the mammalian animals, with TPE-PU-1000 nanoparticles at pH 7.4 for 45 min. Their intracellular distribution was evaluated by CLSM using the same laser and filter setup. The CLSM images of glial cells after incubation with 1×10^{-3} g/mL of TPE-PU-1000 nanoparticles were obtained and illustrated in Fig. S8A. It is obvious that the cell periphery was brighter than other region of the cells, which was similar to that for fixed and permeabilized glial cells stained with commercial Rhodamine Phalloidin (Fig. S8C), indicating the specific interaction between TPE-PU-1000 nanoparticles and microfilament, which is more concentrated along the cell periphery than in the cytosol of glial cells. The specificity of TPE-PU-1000 to microfilaments was further investigated by using commercial Rhodamine Phalloidin to stain the fixed glial cells that were first incubated with TPE-PU-1000 nanoparticles for 45 min at 37 °C (Fig. 3). The transparent grey fluorescence along the cell periphery in Fig. 3D suggested that fluorescence from TPE-PU-1000 and Rhodamine Phalloidin were co-localized in good agreement. The CLSM images shown in Fig. S8A & B indicating that the TPE-PU-1000 nanoparticles had a better performance in living cell subcellular microfilaments imaging in comparison with that commercial Rhodamine Phalloidin. Of note, Rhodamine Phalloidin could not clearly label cytoplasmic actin microfilament systems through directly co-culturing with living cells because organic fluorophore phalloidin conjugates had low living cell membrane permeability (Fig. S8B).[5,28]

To assess the cellular uptake mechanism of the TPE-PU-1000 nanoparticles, we analysed the fluorescence intensity in rat glial cells (Fig. 4) cultured with the same concentration of TPE-PU-1000 nanoparticles for 4 h under different conditions. Quantitative cellular uptake studies showed that the uptake of TPE-PU-1000 by rat glial cells at 4 °C is significantly reduced to 12.4 % (Fig. 4A & B), suggesting that the TPE-PU-1000 nanoparticles entered into rat glial cells via an energy dependent endocytosis pathway. The cellular uptake of the TPE-PU-1000 nanoparticles at 37 °C was equivalent to 106 % and 94 % of the control when rat glial cells were pre-treated with sucrose and genistein (Fig. 4B), two specific endocytic inhibitors for clathrin-mediated and caveolae-mediated endocytosis, suggesting that TPE-PU-1000 nanoparticles were endocytosed through the clathrin- and caveolae-independent energy dependent pathway.[29] Furthermore, the cell viability of rat glial cells remained above 93.4 % after culture with 10^{-3} mg/mL TPE-

View Article Online
DOI: 10.1039/C7CC02555F

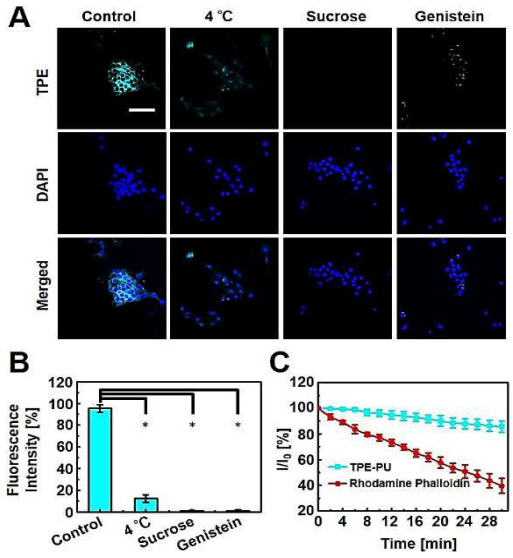

Fig. 4 Analysis of the cellular endocytosis mechanism and photo-stability of TPE-PU-1000. (A) Confocal images of living rat glial cells co-cultured with 1×10^{-3} g/mL TPE-PU-1000 nanoparticles for 4 h under different conditions. Bar scale 20 μm (applicable to all images). (B) Percentages of internalized fluorescence intensity in rat glial cells at 37 °C (control group) or 4 °C or in the presence of sucrose and genistein. (*p < 0.05, *t*-test). (C) Photo-stability comparison between TPE-PU-1000 upon continuous excitation at 364 nm (squares) and Rhodamine Phalloidin upon continuous laser excitation at 543 nm (circles) from 0 to 30 min. I_0 is the initial fluorescence intensity and I is the fluorescence intensity of the corresponding sample after continuous scanning for a designated time interval.

PU-1000 for 48 h, suggesting very low cytotoxicity of the nanoparticles (Fig. S9). The photo-stability of the TPE-PU-1000 in rat glail cells was also studied under continuous laser scanning upon excitation at 364 nm for TPE-PU-1000 and 540 nm for Rhodamine Phalloidin, respectively. As shown in Fig. 4C, TPE-PU-1000 showed ~14.4 % decrease of fluorescence intensity under continuous laser excitation at 364 nm within an observation time of 30 min, while under the same conditions ~40.6 % were observed for Rhodamine Phalloidin. Hence, the results revealed TPE-PU-1000 was promising for long-term cytoplasmic microfilament systems imaging in viable cells.

In conclusion, a novel linear fluorescent block polyurethane copolymer carrying two different polymer blocks and one AIE active fluorophore in the repeating units was synthesized as a long-term subcellular microfilaments imaging probe. This probe take advantages of flexible linear core-shell block molecular structure that enhances cellular uptake and facilitate the specificity binding to the dynamic microfilaments. Visualization of subcellular microfilament systems is achieved via direct co-culturing of the cells with TPE-PU nanoparticles. The TPE-PU nanoparticles are endocytosed through clathrin- and caveolae-independent energy-dependent pathway. As the fluorescence properties and the subcellular microfilaments targeting ability of TPE-PU can be fine-tuned via tailoring the compositions in the repeating units, this study provides a new way of designing fluorescent probes for complicated and dynamic living cell subcellular imaging and detection.

We thank the Natural Science Foundation of China (No.51573097), the Natural Science Foundation of Guangdong Province (No. S2013010013056), Nanshan District Key lab for Biopolymers and safety evaluation (No. KC2014ZDZJ0001A) and Postdoctoral Science Foundation of China (No.2016M592533) for financial support. We also thank Qin-jie Long for assistance with the schematic drawings.

Notes and references

1 E.S. Chhabra, H.N. Higgs, *Nat. Cell Biol.*, 2007, **9**, 1110.
2 D.P. Thomas, A.C. John, *Science*, 2009, **326**, 1208.
3 K. Li, K.Y. Pu, L.P. Cai, B. Liu, *Chem. Mater.*, 2011, **23**, 2113.
4 L. Garcia-Hevia, R. Valiente, R. Martin-Rodriguez, C. Renero-Lecuna, J. Gonzalez. L. Rodriguez-Fernandez, F. Aguado, J. C.Villegas, M. L. Fanarraga, *Nanoscale*, 2016, **8**, 10963.
5 D. Jacot, N. Tosetti, I. Pires, R. J. Stock, A. Graindorge, Y.F. Hung, H.J. Han, R. Tewari, I. Kursula, D. Soldati-Favre, *Cell Host Microbe*, 2016, **20**, 731.
6 E. Betzig, G.H. Patterson, R. Sougrat, O.W. Lindwasser, S. Olenych, J.S. Bonifacino, M.W. Davidson, J. Lippincott-Schwartz, H.F. Hess, *Science*, 2006, **313**, 1642.
7 K.C.W. Wu, C. Y. Yang, C.M. Cheng, *Chem. Commun.*, 2014, **50**, 4148.
8 T. Geng, C. Lu, *Lab Chip*, 2013, **13**, 3803.
9 F. Liu, D. Wu, X.Y. Wu, K. Chen, *Soft Matter*, 2015, **11**, 1434.
10 R. N. Day. M.W. Davidson, *Chem. Soc. Rev.*, 2009, **38**, 2887.
11 K. D. Wegner, N. Hildebrandt, *Chem. Soc. Rev.*, 2015,**44**, 4792.
12 H. Xu, Q. Li, L.H. Wang, Y. He, J. Y. Shi, B. Tang, C.H. Fan, *Chem. Soc. Rev.*,2014, **43**, 2650.
13 H.H. Xiao, G. T. Noble, J. F. Stefanick, R.G. Qi, T. Kizilterpe, X.B. Jing, B. Bilgicer, *J. Control. Release,* 2014, **173**, 11.
14 H.H. Xiao, J. F. Stefanick, X.Y. Jia, X.B. Jing, T. Kiziltepe, Y. Zhang, B. Bilgicer, *Chem. Commun.*, 2013, **49**, 4809.
15 O.S. Wolfbeis, *Chem. Soc. Rev.*, 2015, **44**, 4743.
16 L.F. Feng, C.L. Zhu, H.X. Yuan, LB. Liu, F.T. Lv, S. Wang, *Chem. Soc. Rev.*, 2013, **42**, 6620.
17 S. Huang, S.Y. Liu, K. Wang, C.J. Yang, Y.M. Luo, Y.D. Zhang, B. Cao, Y.J. Kang, M.F. Wang, *Nanoscale*, 2015, **7**, 889.
18 L.P. Heng, W. Qin, S.J. Chen, R.R. Hu, J. Li, N. Zhao, S.T. Wang, B.Z. Tang, L. Jiang, *J. Mater. Chem.B*,2012, **22**, 15869.
19 Y. Yang, X.Y. Wang, Q.L. Cui, Q. Cao, L.D. Li, *ACS Appl. Mater. Interfaces,* 2016, **8**, 7440.
20 L.L. Yan, Y. Zhang, B. Xu, W.J. Tian, *Nanoscale*, 2016, **8**, 2471.
21 Q. Luo, Z.Y. Dong, C.X. Hou, J.Q. Liu, *Chem. Commun.*, 2014, **50**, 9997.
22 B. Bharti, A.L. Fameau, O.D. Velev, *Faraday Discuss.*, 2015, **181**, 437.
23 Z.H.Zhou, G.J. Liu, L.Z, Hong, *Biomacromolecules*,2011,**12**, 813.
24 Y.W. Li, W.B. Zhang, I.F. Hsieh, G.L. Zhang, Y. Cao, X.P. Li, C.; Lotz, B. Wesdemiotis, , H.M. Xiong, S.Z.D. Cheng, *J. Am. Chem. Soc.*, 2011, **133**, 10712.
25 A. Hakonen, J.E. Beves, N. Stromberg, *Analyst.* 2014, **139**, 3524.
26 K.L. Thompson, C.J. Mable, A. Cockram, N.J. Warren, V.J. Cunningham, E.R. Jones, R. Verber, S.P. Armers, *Soft Matter*, 2014, **10**, 8615.
27 G. Zardalidis, J. Mars, J. Allgaier, M. Mezger, D. Richter, G. Fluodas, *Soft. Matter*, 2016, **12**, 8124.
28 S.L. Yao, X. Liu, S.K. Yu, X.M. Wang, S.M. Zhang, Q. Wu, X.D. Sun, H.Q. Mao, *Nanoscale*, 2016, **8**, 10252.
29 L. Li, L. Tian, Y.L. Wang, W.J. Zhao, F.Q. Cheng, Y.Q. Li, B.S. Yang, *J. Mater. Chem. B*, 2016, **4**, 5046.